Universal retraction process of a droplet shape after a large strain jump

S. Assighaou* and L. Benyahia†

Polymères, Colloïdes, Interfaces, UMR CNRS 6120, Université du Maine, Avenue Olivier Messiaen, 72085 Le Mans Cedex 9, France

(Received 28 May 2007; published 11 March 2008)

We evidenced a universal relaxation behavior of a droplet embedded in an immiscible fluid of the same density. After a large strain jump, the relaxation can be characterized by two related relaxation times $\tau_1 = 4.4\tau_2$ independently of the viscosity ratio and of the applied strain. The change in the kinetic process is driven by the drop geometry and happens invariably when the shape of the drop is an oblate ellipsoid of revolution where the relation between the major (L) and the minor (B) axis is given by $\ln(L/B) \approx 0.5$. This universal behavior can be explained by considering the normal stress difference across the droplet interface, i.e., the curvature of the drop.

DOI: 10.1103/PhysRevE.77.036305 PACS number(s): 47.61.−k, 83.50.−v, 82.70.−y

INTRODUCTION

Immiscible fluids that show phase separation and lead to complex morphologies are widely present in various applications. The mechanical properties of liquid emulsions or immiscible polymer blends are not only related to the individual mechanical parameters of each phase in presence but it is known from the initial studies of Taylor [1,2] that geometrical properties can play an important role on the rheological behavior.

Taylor [1,2] first suggested a relation between geometrical characteristics and rheology of liquid immiscible blends by considering a simple model system: an isolated drop embedded in a matrix of another liquid subjected to a flow. He proposed to relate the size anisotropy of the deformed drop to the capillary number $Ca = r_0 \eta_m \dot{\gamma}/\Gamma$ and the viscosity ratio $K = \eta_d/\eta_m$ (where η_d and η_m are, respectively, the Newtonian viscosity of the drop and the matrix, r_0 is the initial radius of the drop, Γ is the interfacial tension, and $\dot{\gamma}$ is the shear rate). The capillary number corresponds to the ratio of viscous and surface tension forces.

Since the first work of Taylor [1,2], many authors were interested in the study of drop deformations. The most outstanding results, before 1994, are summarized by Grace [3], Rallisson [4], and Stone [5], to name a few. The burst of drops during [6,7] or after having stopped a constant shear rate flow [8,9] was in the foreground. Some work concerned the shape relaxation of a slightly deformed drop [10–15] but, as far as we are aware, not much work has been done for the case of large deformations.

Submitted to a strain step γ_0, a drop increases its length L and decreases its width B in the gradient/velocity plane (Fig. 1). After the step strain the drop shape relaxes back by decreasing L and increasing B to reach a spherical shape. For small deformations [14,16], the drop deforms slightly from a spherical shape to an ellipsoidal shape. In that case, the Henky strain of the principal axis of the ellipsoid, defined as $\ln(L/2r_0) = \ln(\lambda_L)$, where λ_L is the principal stretching ratio of the drop, tends towards zero with an exponential decay of a characteristic relaxation time τ_2:

$$\ln(\lambda_L) \propto \exp\left(-\frac{t}{\tau_2}\right). \tag{1}$$

τ_2 can be derived [17] from Palierne's [18] emulsion model and depends simply on K for clean interfaces, i.e., without surfactant or impurities:

$$\tau_2 = \frac{\tau_{Ca}}{4}\frac{(19K+16)(2K+3)}{10(K+1)}. \tag{2}$$

$\tau_{Ca} = \eta_m r_0/\Gamma$ is the capillary time of the drop. In particular, the retraction of a slightly deformed drop is used to determine the interfacial tension of polymer blends in the molten state (see Refs. [14,17], for example). In practice, the drop deformation should be enough to obtain accurate values while keeping the drop in its ellipsoidal shape which is the principal limit of this method [19]. For highly stretched droplets, the dynamics of retraction is still not clearly explained in the literature: see, for example, Refs. [20–22].

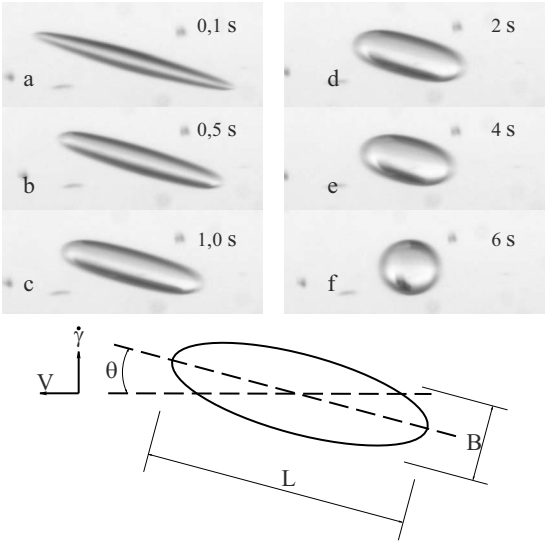

FIG. 1. Snapshot of a single PU drop in a PDMS matrix during a shape relaxation after a step strain. $\gamma_0 = 2$ and $K = 0.01$. The time of each image is indicated within the figure. The bottom figure represents a sketch of a drop, with the characteristic dimensions, while deformed in a driving flow.

*souad.assighaou@univ-lemans.fr
†lazhar.benyahia@univ-lemans.fr

In this paper we focus on the behavior of the drop retraction after a large strain step. In particular, we evidenced a universal kinetic process during the relaxation of the drop shape and we propose an explanation based on the reduction of the droplet-matrix interface curvature.

EXPERIMENTAL METHODS

The strain step which induced the drop deformations was generated by a counter-rotating shear device designed in the laboratory [23,24]. The liquid was placed between two glass disks attached to two counter-rotating motors. All the measurements were carried out at constant temperature $T=20\ ^{\circ}\mathrm{C}$. A charge coupled device (CCD) camera imaged the drop during its retraction. The CCD camera and the motors are monitored using home-developed software under a LabView environment. Image analysis software (ImaqVision) was used to measure the principal lengths of the drop (major axis L and minor axis B) and its orientation angle θ relative to the velocity direction in the velocity-gradient plane.

The materials used in this study were polydimethylsiloxane (PDMS) for the continuous phase and polyurethane (PU) for the dispersed phase. Two PDMS samples, supplied by Rhodia, were used in this work: 48V30000 ($\eta=32.5$ Pa s) and 48V100000 ($\eta=100$ Pa s). Polyurethanes were obtained by polycondensation of [poly(oxypropylene)diol] with hexamethylene diisocyanate (HMDI) in the presence of dibutylt etin dilaurate as a catalyst. The synthesis procedure was described by Prochazka *et al.* [25]. PU was chosen for three reasons. First, we can adjust the viscosity of the drop, i.e., the polyurethane, by varying the stoichiometric ratio between isocyanate groups and hydroxyl groups ($\eta=[0.485-132$ Pa s]). Therefore almost 3 decades of $K=[0.01-4.09]$ were explored. Second, the interfacial tension for the whole droplet-matrix couple is well-defined since the precursor is the same for the different polyurethanes. Finally, we obtain clean interfaces since the synthesis is carefully controlled.

Zero shear viscosity of the used materials was measured in a steady state flow using a stress controlled rheometer (AR1000-TA Instruments) equipped with a cone/plate geometry (diameter 25=mm, cone angle=0.035 rad). The temperature was fixed at 20 °C. In the accessible range of the shear rates ($\leqslant 100\ \mathrm{s}^{-1}$), both PU and PDMS can be considered as Newtonian liquids. In addition, the terminal relaxation times for the used samples, estimated from the frequency dependence of the shear moduli, are less than 1 ms. Thus for the present system the intrinsic relaxation times of the liquids are orders of magnitude faster than the drop relaxation time.

RESULTS

After applying an external step strain (γ_0) to the continuous phase, the drop slanted along the flow direction with an angle θ which remained unchanged during the whole relaxation process as it was reported earlier [26]. If we increase the amplitude of γ_0, the drop takes an "eyelike" shape [Fig. 2(a)] at the first moment of its deformation. It looks like a modified prolate ellipsoid where the extremities form tips as already reported [4,6,8,26]. The relaxation of the eyelike shape starts by losing rapidly the acuteness of its extremities and then by swelling perpendicularly to its principal axis, so that it tends to adopt a cylinderlike shape with spherical ends [Fig. 1(c)] (see Ref. [26], for example). The time during which the drop adopts an eyelike shape is small in comparison to the one during which it adopts the form of a spherocylinder (less than 10%). Afterward, the retraction of the spherocylinder is considered as the first step of the drop shape relaxation.

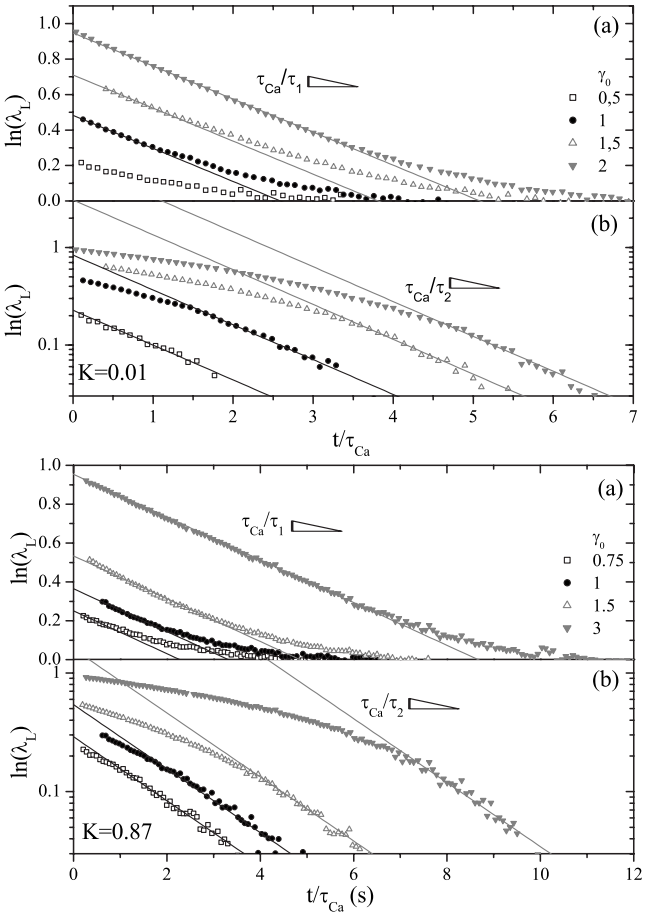

FIG. 2. Henky strain of the principal axis of a PU drop in a PDMS matrix for two K during the retraction process after a step strain (indicated in the figure). The two representations of the same data are showmen to emphasize the two relaxation processes. The symbols represent experimental results. The straight lines represent linear (a) and exponential decay (b), respectively, for the first and the second relaxation processes.

During the second step, the drop has an ellipsoidal-like shape (Fig. 1) and the major axes decreases until the drop reaches its spherical equilibrium shape at the end of the relaxation process [Fig. 1(f)]. Furthermore, these two approximations on the drop shape, i.e., ellipsoidal and spherocylinder, give a constant value of the drop volume with a margin of 10%.

By plotting the Henky strain of the principal axis of the drop one can distinguish the two successive relaxation steps

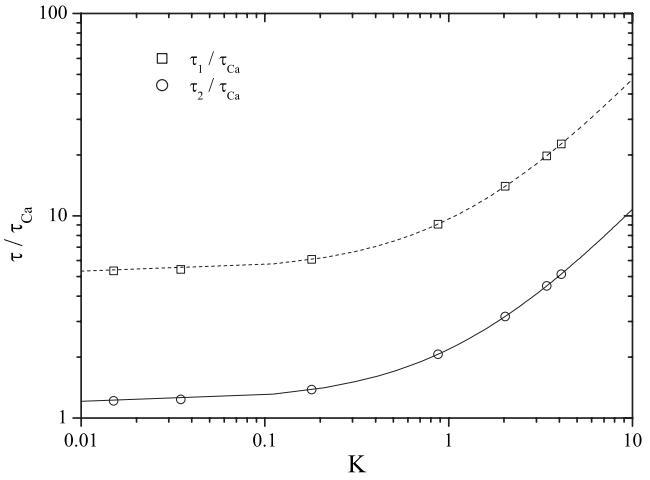

FIG. 3. Evolution of the two relaxation times τ_1 and τ_2, normalized by the emulsion time τ_{Ca}, versus K. The solid line represents the prediction of the Palierne model [Eq. (2)]. The dashed line represents Eq. (2) multiplied by 4.4.

(Fig. 2). First, for small deformations, i.e., when the drop remains ellipsoidal, $\ln(\lambda_L)$ exhibits an exponential decay with characteristic relaxation time τ_2 [Eq. (1)]. This time appears to be independent of γ_0, in agreement with previous experimental results [10,11,16,17] and with the theoretical prediction of Palierne [18]. Indeed, according to Palierne's work [18], τ_2 can be expressed by Eq. (2) for dilute emulsions, i.e., without drops interactions. The perfect agreement between the present results and the prediction of Eq. (2) is shown in Fig. 3. This shows that the interface is clean and without unspecified elasticity which would be induced by a surfactant or other impurities. The interfacial tension than can be derived from τ_2 is about 4.5 mN/m which is in good agreement with results given by the pendent drop method.

At the first step of the relaxation when the drop is highly deformed and exhibits a cylindrical-like shape, $\ln(\lambda_L)$ decreases linearly with a characteristic time τ_1:

$$\ln(\lambda_L) \propto -\frac{t}{\tau_1}. \tag{3}$$

τ_1 follows the prediction of Eq. (2) but is slightly shifted towards higher values. In fact, τ_1 is simply proportional to τ_2 by a prefactor independent of γ_0 and K: $\tau_1 = 4.4\tau_2$ (Fig. 3).

Another noticeable result is the transition between the two relaxation processes. In fact, the transition from the fast relaxation process, where the drop is like a cylinder with spherical ends, to the slow relaxation process, where the drop adopts an ellipsoidal shape, occurs for the same value of $\ln(\lambda_L) \approx 0.34$ independently of K and γ_0 [Fig. 2(a)]. Consequently, we can obtain, for each K, a master curve (Fig. 4) of $\ln(\lambda_L)$ versus time, normalized by τ_{Ca}, simply by subtracting an arbitrary constant (d) which depends on γ_0 and K. Details of this dependence will be discussed elsewhere.

DISCUSSION

What accounts for this universal behavior? Two hypotheses could be envisaged: (1) the drop reduces its surface in order to minimize the interfacial forces, and (2) the drop reduces its curvature and tends to reach a uniform state by taking a spherical shape.

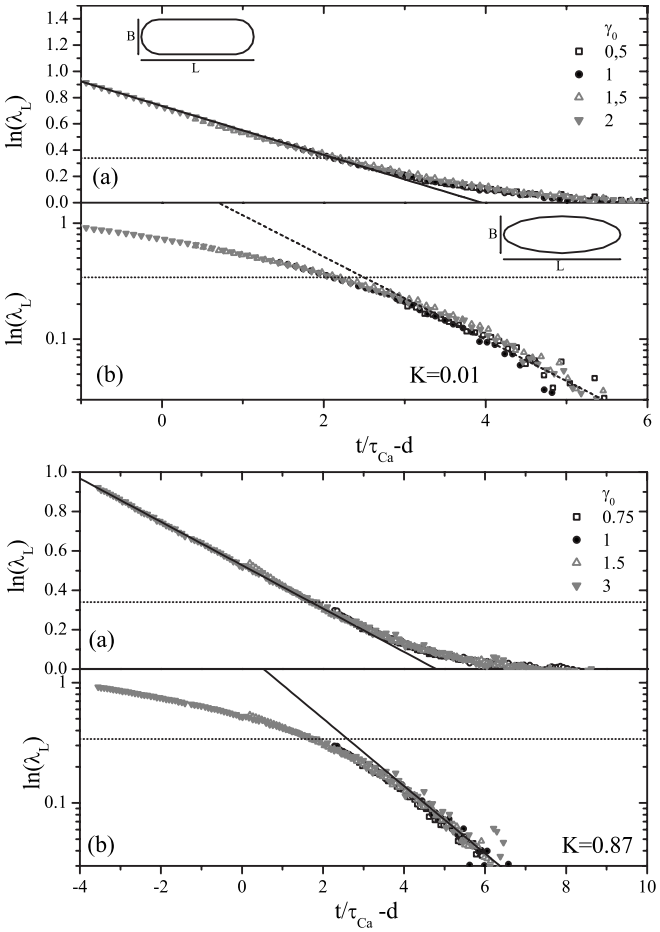

FIG. 4. Master curves of the Henky strain of the principal axis of a PU drop in a PDMS matrix for two K during the retraction process. The experimental conditions are the same as in Fig. 2. The straight lines represent the first (a) and the second (b) relaxation process. The dotted line shows the critical transition value $[\ln(\lambda_{Li}) = 0.34]$ between the first and the second relaxation regime.

Let us consider, as a first approximation, a drop as an axisymmetric ellipsoid at low deformation and as a cylinder with spherical extremities at large deformation. For these two geometrical assumptions, we consider a symmetry axis along L.

Since both fluids are considered as incompressible, the volume of the drop remains unchanged during the relaxation process. Taking the conservation of the volume of the drop as a constraint, we can deduce the ratio of the area of the deformed drop normalized by the surface area of the spherical undeformed drop. We find:

$$A_e = \frac{1}{2}\left[\frac{B^2}{4r_0^2} + \frac{2r_0}{B\sqrt{1-\frac{B^6}{64r_0^6}}}\arcsin\sqrt{1-\frac{B^6}{64r_0^6}}\right]$$

and

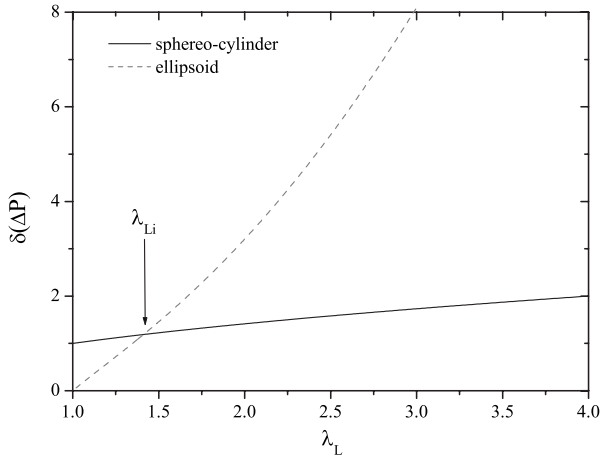

FIG. 5. Pressure gradient as a function of the principal stretching ration of the principal axis of the drop. The data correspond to values calculated combining Eq. (7) for the spherocylinder shape and Eq. (8) for the ellipsoidal shape.

$$A_c = \frac{r_0}{3B} + \frac{B^2}{12r_0^2} \tag{4}$$

for the ellipsoid and the spherocylinder, respectively. The difference $A_e - A_c$ is always positive whatever the stretching ratio. The argument based on the minimization of the interfacial area between the drop and the continuous medium, proposed by different authors [26], can neither explain the shape of the drop nor the transition value because the area of the ellipsoid is always larger than that of the spherocylinder.

We suggest another hypothesis related to the evolution of the drop curvature. In other words, we consider that the key factor in the relaxation process of the drop is related to a decrease of the curvature gradient at the interface. Indeed, the pressure difference ΔP across a curved interface between two liquid phases is given by the Laplace law:

$$\Delta P = P_i - P_e = \Gamma\left(\frac{1}{R_1} + \frac{1}{R_2}\right). \tag{5}$$

P_i and P_e are the pressures on both sides of the interface, and R_1 and R_2 are the principal algebraic curvature radii of the interface at the considered point (the excess pressure is on the side of the interface where the center of the curveted is). Departing from its spherical shape, the drop undergoes changes in its local algebraic curvatures. We assume that the drop relaxation is controlled by the changes in its curvature which involve nonuniform ΔP along the deformed surface of the drop. The nonconstant internal pressure is related to internal convection. In fact, during its relaxation, internal convection tends to decrease the internal gradient of pressure ΔP in order to approach the equilibrium state. At equilibrium, there is zero internal flux and ΔP is constant. The spherical shape is then recovered.

Let us consider, as a first approximation, only the two extremes of ΔP which, of course, will depend on the drop geometry. The difference between these two values will be considered as an approximation of the gradient of ΔP, called $\delta(\Delta P)$.

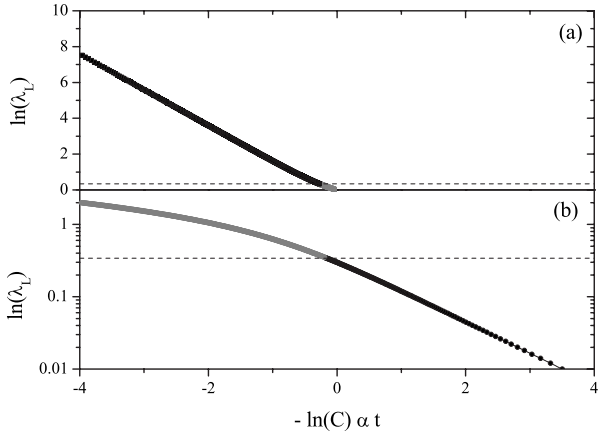

FIG. 6. Henky strain of the principal axis of the drop versus time, respectively, for large deformation (a) and small deformation (b).

Based on the video observation, mentioned previously, we consider two shapes of the drop: (1) a cylinder with two spherical extremities, called spherocylinder, during the first step of the relaxation process of the drop [sketch in Fig. 4(a)] and (2) an axisymmetric ellipsoid during the second step of the relaxation process of the drop [sketch in Fig. 4(b)]. This model can certainly be improved but this simple assumption is sufficient to explain the main observations.

The maximum variation of P is proportional to $C_1 - C_2$. C_1 and C_2 are, respectively, the highest and the lowest value of the deformed drop curvature normalized by the initial radius r_0,

$$\delta(\Delta P)_n = \Gamma C = \Gamma(C_1 - C_2). \tag{6}$$

Therefore $\delta(\Delta P)$ can be described by Eqs. (7) and (8), respectively, for the spherocylinder and the axisymmetric ellipsoid,

$$\delta(\Delta P) \propto C_C = \frac{1}{\lambda_B} \quad \text{with } \lambda_L = \frac{2+\lambda_B^3}{3\lambda_B^2}, \tag{7}$$

$$\delta(\Delta P) \propto C_e = \frac{2-\lambda_B^3(1+\lambda_B^6)}{2\lambda_B^4} \quad \text{with } \lambda_L = \frac{1}{\lambda_B^2}, \tag{8}$$

λ_B is the stretching ratio of the minor axis of the drop defined as $B/2r_0$.

Figure 5 represents the evolution of $\delta(\Delta P)$ versus λ_L for the two considered morphologies. For large deformations ($\lambda_L > \lambda_{Li}$), $\delta(\Delta P)$ for the spherocylinder is lower than the one for the ellipsoid of revolution. Therefore the spherocylinder is the privileged shape. For small deformations ($\lambda_L < \lambda_{Li}$), $\delta(\Delta P)$ is smaller for the ellipsoid of revolution and the ellipsoid of revolution is the privileged shape. According to this argument, we can understand the origin of the change in the shape of the drop during the retraction process. The critical transition value λ_{Li} is obtained by equalizing the expressions of C_c [Eq. (7)] and C_e [Eq. (8)]. This leads to

$\ln(\lambda_{Li}) \approx 0.34$ which is equal to the experimental value where the change in the relaxation process happens. It follows that $\ln(Li/Bi) \approx 0.5$.

We can also understand the kinetics of the retraction process by considering the interface curvature of the deformed drop. Indeed, we suppose that $\delta(\Delta P)$ decays exponentially with a characteristic time τ_P which depends on the polymer. This assumption is reasonable since we know that almost all polymers relax in this way.

$$\delta(\Delta P) \propto e^{-t/\tau_p} \quad \text{or } C \propto e^{-t/\tau_p}. \tag{9}$$

Combining Eqs. (7)–(9) leads to the dependence of $\ln(\lambda_L)$ shown in Figs. 6(a) and 6(b), respectively, for large and small deformations. One can distinguish, when the drop adopts a spherocylinder shape, the Henky strain of the principal axis of the drop decays linearly. When a drop adopts an ellipsoidal shape, $\ln(\lambda_L)$ presents an exponential decay.

In conclusion, the gradient of the curvature of the interface which is directly related to Laplace's pressure determines the drop retraction. The relaxation of a drop after a strain jump is a simple geometrical process. The morphology transition as well as the kinetics of the drop retraction can be simply explained by the geometry of the interface.

ACKNOWLEDGMENTS

It is a pleasure to thank J.F. Palierne, J. Rajchenbach, and T. Nicolai for fruitful discussions. This work was supported by the Conseil Régional des Pays de Loires.

[1] G. I. Taylor, Proc. R. Soc. London, Ser. A **138**, 41 (1932).
[2] G. I. Taylor, Proc. R. Soc. London, Ser. A **146**, 201 (1934).
[3] H. P. Grace, Chem. Eng. Commun. **14**, 225 (1982).
[4] J. Rallison, Annu. Rev. Fluid Mech. **16**, 45 (1984).
[5] H. A. Stone, Annu. Rev. Fluid Mech. **26**, 95 (1994).
[6] B. Bentley and L. Leal, J. Fluid Mech. **167**, 241 (1986).
[7] A. Acrivos and T. S. Lo, J. Fluid Mech. **86**, 641 (1978).
[8] H. A. Stone and L. G. Leal, J. Fluid Mech. **198**, 399 (1989).
[9] H. A. Stone and L. G. Leal, J. Fluid Mech. **206**, 223 (1989).
[10] M. Tjahjadi, H. A. Stone, and J. M. Ottino, J. Fluid Mech. **243**, 297 (1992).
[11] M. Tjahjadi, J. M. Ottino, and H. A. Stone, AIChE J. **40**, 385 (1994).
[12] D. C. Tretheway, J. Non-Newtonian Fluid Mech. **99**, 81 (2001).
[13] W. Lerdwijijarud, R. G. Larson, A. Sirivat, and M. J. Solomon, J. Rheol. **47**, 37 (2003).
[14] S. Guido and M. Villone, J. Colloid Interface Sci. **209**, 247 (1999).
[15] V. Sibillo, M. Simeone, S. Guido, F. Greco, and P. L. Maffettone, J. Non-Newtonian Fluid Mech. **134**, 27 (2006).
[16] I. Sigillo, L. d. Santo, S. Guido, and N. Grizzuti, Polym. Eng. Sci. **37**, 1540 (1997).
[17] A. Luciani, M. Champagne, and L. Utracki, J. Polym. Sci., Part B: Polym. Phys. **35**, 1393 (1997).
[18] J. Palierne, Rheol. Acta **29**, 204 (1990).
[19] P. Xing, M. Bousmina, D. Rodrigue, and M. Kamal, Macromolecules **33**, 8020 (2000).
[20] A. Cohen and C. J. Carriere, Rheol. Acta **28**, 223 (1989).
[21] C. J. Carriere, A. Cohen, and C. B. Arends, J. Rheol. **33**, 681 (1989).
[22] K. Moran, A. Yeung, and J. Masliyah, J. Colloid Interface Sci. **267**, 483 (2003).
[23] S. Assighaou, Ph.D. thesis, Université du Maine, 2006 (unpublished).
[24] S. Assighaou, G. Pavy-Le Du, and L. Benyahia, Rhéologie **11**, 45 (2007).
[25] F. Prochazka, T. Nicolai, and D. Durand, Macromolecules **33**, 1703 (2000).
[26] H. Yamane, M. Takahashi, R. Hayashi, and K. Okamoto, J. Rheol. **42**, 567 (1998).